IUST
Iran University of Science and Technology

Iranian Journal of Electrical and Electronic Engineering

Journal Homepage: ijeee.iust.ac.ir

Calculation and Analysis of the Electric Field of the OIP Bushings under Internal Humidity and Surface Polluted Conditions using FEM

Mohammad Abouhosseini Darzi*, Mohammad Mirzaie*(C.A.), Amir Abbas Shayegani Akmal** and Ebrahim Rahimpour***

Abstract: Bushings are one of the most important components of electrical equipment such as power transformers, reactors, capacitors. Most of the installed bushings have Oil-Immersed Paper (OIP) insulation structure. Bushing failure is caused by various reasons such as poor manufacturing process, overloading and also poor installation process, but moisture ingress is one of the main reasons of OIP bushing defect during its operation. In this paper, the electric field distribution of OIP bushings in multiple situations are simulated and effects of moisture distribution are analyzed. The simulations are stablished in polluted and clean surfaces of the studied bushing and done by COMSOL Multiphysics Software. The results show that non-uniform moisture distribution has a significant effect on electric fields of OIP insulation. This effect strongly increases with increasing the pollution on the external insulator of the bushing.

Keywords: Finite Element Method (FEM), Moisture, OIP Bushing, Pollution, Transformer

1 Introduction

THE Power transformers are one of the most important and expensive equipment of power system. According to statistics, one of the most important causes of the accidents on power transformers is the bushing [1-3]. Also, as reported in [1], the main source of fire accidents in transformers is bushing. Bushings are equipment that doesn’t have any protection, so if any failure occurs in their internal insulation system, it will lead to explosion. The structure of most high voltage bushings is condenser type. This type of bushings includes some aluminum foils wounded around the core cylindrical and make multiple capacitors to homogenize the electric field in the bushing [3].

The main insulation system of the most of the bushings that are installed on transformers is Oil-Immersed Paper (OIP). Because of paper in OIP bushing insulations, the moisture has tendency to penetrate into this type of bushings. In the transformer's oil-paper insulation system, the moisture absorption ability of insulating paper is approximately 104 times stronger than insulating oil, and the vast majority of moisture exists in the insulation paper when the moisture in the oil-paper insulation system is in equilibrium [2]. For condenser bushing, the thickness of insulation paper is thinner than that of insulating paper in transformers and the moisture absorption ability is stronger. So, the moisture is almost completely concentrated in the insulation paper, and will be accelerated the insulation aging process [2]. The main source of moisture is from oil leakage through gaskets [4]. Besides, the aging process can increase the moisture in the bushing insulation system. Moisture is one of the most destructive features of the bushings. It can cause partial discharges and electric arcs inside the bushing. Moisture in OIP insulation system has a diffusion nature and move from paper to oil and vice versa by the

Iranian Journal of Electrical & Electronic Engineering, 2025.
Paper first received 09 Aug. 2024 and accepted 17 Mar 2025.
* The authors are with the Department of Electrical & Computer Engineering, Babol Noshirvani University of Technology, Babol, Iran.
E-mail: md.abouhosseini@stu.nit.ac.ir , mirzaie@nit.ac.ir.
** The author is with the Department of Electrical Engineering, University of Tehran, Tehran, Iran.
E-mails: shayegani@ut.ac.ir.
*** The author is with the Institute of Electrical Power Engineering and High Voltage Technology, THWS, Schweinfurt, Germany.
E-mails: ebrahim.rahimpour@thws.de.
Corresponding Author: M. Mirzaie.

temperature changes [5]. Also, moisture distribution is related with the time of penetration. In the early times, the moisture distribution of the bushing is non-uniform, but over the time, the moisture distribution changes and becomes uniform [6]. As the importance of the electric field changes in the bushing internal insulation [7], in this study, the effect of the moisture on the maximum electric field is investigated. The issue of the moisture in bushing insulation has been investigated in some papers, but most of them are related to measurement and estimation of the moisture [8-10]. In [9], the effect of moisture distribution on the bushing has been studied, but these investigations were on the frequency domain spectroscopy (FDS) curve. [11] has investigated the effect of the moisture on the electric field, but in that study, only the changes on the dielectric permittivity have been studied and the changes on the conductivity have not been considered. Similarly, in [12] the moisture distribution effect on the internal fields of bushings have been assessed, but they didn't aspect the electrical conductivity changes on their assessment. The effects of moisture on bushings have been experimentally evaluated in [7], but its impact on the electric field has not been considered.

Since the bushings are external equipment, there is a possibility of pollution on its outdoor insulator, especially in industrial environments. As the pollutions make conductive layers on the surface of bushing, and they can affect on the electric field distribution. The number of articles that have examined the effect of pollution on the bushings is very small. In [13-15], the effect of pollution on the bushing insulators has been investigated, but these investigations were mainly studied on the external field of bushing. In [16] the environment effects on the bushings have been evaluated but the bushing was a SF6 tank type bushing.

However, the electric field evaluation of a practical insulation is so complex that an analytical method is very difficult, if not possible, to compute the exact solutions. Numerical methods such as Finite Element Method (FEM) are thus often adopted in engineering applications to derive acceptable solutions [17].

In this paper, the internal electric field of the power transformers bushing under two operational conditions such as moisture and insulator pollution has been investigated by FEM method. In the previous studies didn't perform a complete assessment on the moisture distribution effect but, in this paper, the effects of moisture distribution on the electric field of OIP bushings are simulated and analyzed. For better evaluating this issue, it is assumed the moisture enters the bushing through the flange and gradually penetrates to the inner layers. This issue is investigated in 8 scenarios or stages, which the last stage is uniform moisture distribution. So, the difference between the uniform and un-uniform distribution of the moisture in the bushing insulation is also discussed. Also, no study has been conducted on the effects of external surface contamination on the internal field of the bushings, so, in this study, analysis of bushing insulation under surface polluted and non-polluted conditions have been done. For defining the level of contamination, the IEC standard has been used. Besides, the effects of the internal moisture and the external pollution on electric field of the bushing have been evaluated simultaneously. In this study, the temperature of bushing insulation system insulation system is assumed uniform and equals to ambient temperature (20°C). The studied bushing is an 145kV OIP bushing with porcelain insulator, and the simulations has been done by COMSOL Multiphysics software based on finite element method (FEM).

2 Methodology

2.1 Moisture Distribution in OIP Bushings

Moisture in the insulating papers tends to diffuse and distribute uniformly throughout the material. Moisture diffusion in the insulation can be estimated from Fick's second law [10]. This law is expressed by this equation:

$$\frac{\partial \mathrm{C_{paper}}}{\partial \mathrm{t}} = \nabla.\left[(\mathrm{D_r} + \mathrm{D_z})\nabla \mathrm{C}\right] \tag{1}$$

Where C is the local moisture concentration and Dr, Dz are diffusion factors along radial and axial directions, and t is the diffusion time. In the condenser bushings because of aluminum foils, the speed of moisture diffusion at radial direction is lower than axial, so it takes long time (many days) to get uniform [18]. According [10], diffusion factor can be calculated by an empirical relationship that is shown here:

$$\mathrm{D}\left(\mathrm{C_{paper}}, \mathrm{T}\right) = \mathrm{D_0}\exp[\mathrm{kC_{paper}} + \mathrm{E_a}(1/\mathrm{T_0} - 1/\mathrm{T})] \tag{2}$$

Where D is diffusion factor and T is the experimental temperature in Kelvin and Ea is the activation energy of the diffusion process (8074 J/K) and D0 = 1.34 × 10−13 m2/s, k = 0.5 and T0 = 298 K.

For analyzing the moisture effects on dielectrics, the changes of its properties have to be assessed. As the bushings main insulation is OIP, the evaluation has been on the main electric properties of OIP. For electric studies, the important parameters of insulations are electric conductivity (σ) and dielectric relative permittivity (εr). Both of these properties are affected by the moisture of dielectric system, but conductivity is much more sensitive than permittivity [19]. The relation between moisture content of OIP has been extracted by an experimental work as Fig. 1 [11].

According to this curve (Fig. 1), the relative permittivity of oil-immersed insulation paper can be estimated approximately by its moisture content percentage (mc) as Eq. 3 shows [11]. The moisture content percentage (mc) means the total water weight in layer divided by total paper weight in each layer.

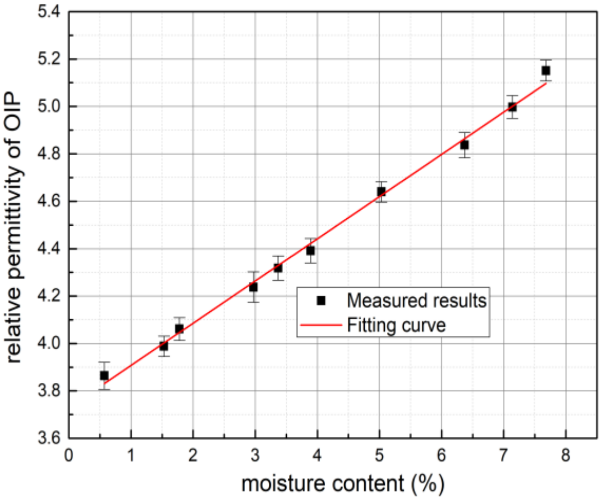

Fig 1. Measured and fitted results of relative permittivity for oil-immersed insulation paper with different moisture contents [11]

Based on Eq. (3), as the water content inside the OIP increases, the permittivity also increases; This is due to the polar nature of water molecules. Water has a high permittivity, and when moisture infiltrates insulation materials, it introduces additional dipolar polarization. This added polarization enhances the material's overall permittivity [4].

$$\varepsilon_r = 3.73 + 0.18 \times mc \qquad (3)$$

But electric conductivity relation is more complicated, because of frequency dependence of this property. For calculating the conductivity, the modified Havriliak–Negami (HN) model has been used [20]. In this model, the complex permittivity of an oil-paper dielectric is related to paper moisture content by this equation [12]:

$$\varepsilon^*(\omega) = \varepsilon_\infty + \frac{\varepsilon_s - \varepsilon_\infty}{(1+(j\omega\tau)^\alpha)^\beta} \qquad (4)$$

$$\begin{cases} \varepsilon'(\omega) = \varepsilon_\infty + \dfrac{\Delta\varepsilon\cos(\beta\theta)}{\left(1+2(\omega\tau)^\alpha\cos\left(\frac{\alpha\pi}{2}\right)+(\omega\tau)^{2\alpha}\right)^{\beta/2}} & (5) \\ \varepsilon''(\omega) = \dfrac{\Delta\varepsilon\sin(-\beta\theta)}{(1+2(\omega\tau)^\alpha\cos(\alpha\pi/2)+(\omega\tau)^{2\alpha})^{\beta/2}} + \dfrac{\sigma_{DC}}{\varepsilon_0\omega} \end{cases}$$

where ω is the angular frequency, εs is the static permittivity (low-frequency), ε∞ the permittivity at the high-frequency limit, τ is the relaxation time, α and β are parameters reflecting the distribution of relaxation time, and they are between 0 and 1. Δε is the difference between the εs and ε∞, and σDC is the DC conductivity and θ a parameter which has the following expression [12]:

$$\theta = \arctan\left[\frac{(\omega\tau)^\alpha\sin(\alpha\pi/2)}{1+(\omega\tau)^\alpha\cos(\alpha\pi/2)}\right] \qquad (6)$$

$$\begin{cases} \Delta\varepsilon = 0.85\exp(mc/0.98) + 0.22 \\ \beta = 0.33 + 0.05mc \\ \tau = 886.13 \times mc^{-0.84} \\ \sigma_{DC} = 1.5 \times 10^{-11} \times \exp(mc/0.99) + 4.88 \times 10^{-11} \end{cases} \qquad (7)$$

Based on relations between insulations electric field (E) and current density (J), the electric conductivity (σ) can be extracted from Equations (8) to (11). As shown in Equation (8), the current density can be separated into charge current density (Je) and loss current density (Jσ), and also can be expressed by complex relative permittivity (Eq. 9). From relations Eq. 8 and Eq. 9 and complex permittivity equation (Eq. 10), the complex relative permittivity can be extracted (Eq. 11) and the electric conductivity can be obtained (Eq. 12) [13]:

$$J = J_e + J_\sigma = j\omega\varepsilon_0\varepsilon_r E + \sigma E = j\omega\varepsilon_0\left(\varepsilon_r - j\frac{\sigma}{\omega\varepsilon_0}\right)E \qquad (8)$$

$$J = j\omega\varepsilon_0\varepsilon_r^* E \qquad (9)$$

$$\varepsilon^* = \varepsilon' - j\,\varepsilon'' \qquad (10)$$

$$\varepsilon' = \varepsilon_r \quad , \quad \varepsilon'' = \frac{\sigma}{\omega\varepsilon_0} \qquad (11)$$

$$\sigma = \omega\varepsilon_0\varepsilon'' \qquad (12)$$

Based on the Equations (12) and (5), the electric conductivity can be calculated from paper moisture content as shown below:

$$\sigma = \frac{\omega\varepsilon_0\Delta\varepsilon\sin(-\beta\theta)}{(1+2(\omega\tau)^\alpha\cos(\alpha\pi/2)+(\omega\tau)^{2\alpha})^{\beta/2}} + \frac{\sigma_{DC}}{\varepsilon_0\omega} \qquad (13)$$

2.2 Pollutions effects

The surface pollution effects on the insulators are considered as a thin layer along the bushing external surface [14]. Electric field along the insulator surface can be calculated directly from the potential distribution [15]:

$$E = -\nabla V \qquad (14)$$

Maxwell's equation could be used to calculate the change in electric field:

$$\nabla . E = \frac{\rho}{\varepsilon} \qquad (15)$$

Where ρ and ε are the free charge density and dielectric constants of material respectively. Equations (14) and (15) can be combined to obtain the Poisson's equation [8]:

$$-\nabla.(\nabla V) = \frac{\rho}{\varepsilon} \qquad (16)$$

Poisson's equation will become a Laplace equation if there is no space charge [21]:

$$\nabla^2 V = 0 \qquad (17)$$

The pollution layer is modelled as a conductive layer and the conductivity of this layer change to simulate the effect of pollution severity level. For defining the severity level of pollution, IEC60815-1 standard is used. In this standard, the pollutions are categorized to 5 classes (very light, light, medium, heavy, very heavy) [22]. According to these classes, some conductivities are assumed from 1 S/m to 1 μS/m for the pollution layer.

Based on the Conservation law that governs the conductive layer, it can be expressed as follows [23]:

$$\nabla . J_v + j\omega(\nabla . D) = 0 \tag{18}$$

Where J_v is the volume current density (A/m2) and D is the electric flux density (C/m2) and ω is the angular frequency (rad/s). The current density can be written in term of electric field in equation Eq. 19, and by replacing equations in Eq. 18, the main equation (Eq. 20) can be obtained, where σ_v is volume conductivity (S/m) and ε is permittivity (F/m).

$$\nabla . J_v = \nabla . (J_e + J_\sigma) = \nabla . (\sigma_v E + j\omega\varepsilon E) = \nabla . ((\sigma_v + j\omega\varepsilon)E) \tag{19}$$

$$(\sigma_v + j\omega\varepsilon)\nabla^2 V + j\omega\rho_s = 0 \tag{20}$$

According to some researches, the surface charge density (ρ_s) along the insulator can be considered equal zero, so it results to solving a modified Laplace's Equation [24], [25]:

$$(\sigma_v + j\omega\varepsilon)\nabla^2 V = 0 \tag{21}$$

Equation (21) will be used as a boundary condition in the pollution domain.Illustrations

3 Bushing model simulation

In this study, a sample 145kV OIP bushing (line voltage) has been modelled in COMSOL Multiphysics software. The bushing has 12 layers with geometries as described in Table 1 [26]. The layers are made from papers that wounded around main rod of bushing. These layers are separated with cylindrical aluminum foils and the last foil is grounded by attaching to the bushing flange. The external insulator is assumed porcelain and designed to be installed on power transformers. Because of symmetry structure of bushings and in order to decrease the processing time and complexity of simulations, a two-dimensional (2D) axisymmetric model is considered according to Fig. 2.

As the electric field in vertical direction of the bushing internal insulation usually is approximately constant [7], in this study, only the electric field changes in radial direction of that is investigated.

Table 2 shows the electric properties of the material used in this simulation [26]. The simulations have been performed in frequency domain with 50Hz frequency, and the electric current physic has been used.

Table 1. Specification of the aluminum foils [26]

Foil number	Spacing between rod and foils (mm)	Length of foils (mm)
1	30	1900
2	41	1728
3	52	1390
4	63	1169
5	74	1007
6	85	880
7	96	787
8	107	711
9	118	647
10	129	594
11	140	549
12	151	510

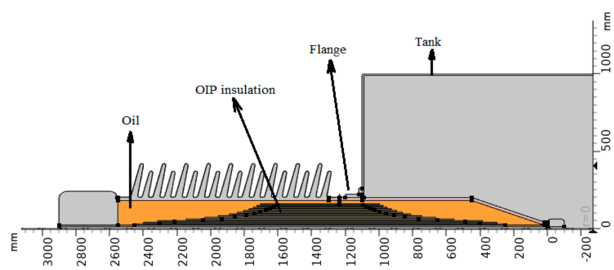

Fig 2. Bushing model geometry

Table 2. Dielectric properties for the studied bushing [26]

Material	Relative permittivity (ε_r)
Air	1
Porcelain	5.5
Oil	2.2
OIP	4
Aluminum	10^8

4 Simulation Results and discussion

In this section, based on the equations presented in section two, the simulations were established on the studied bushing model. In these simulations, the studied bushing is analyzed in two conditions; the first one is under high moisture and the other is under the high pollution. The Fig. 3 shows the potential and electric field distribution along the radial direction (from rod to the last foil) under normal condition without any moisture and external pollution.

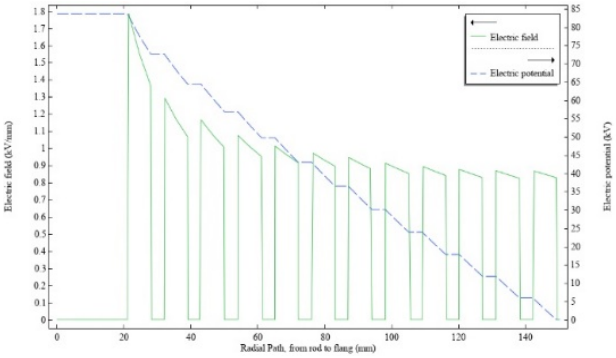

Fig 3. Electric potential and field distribution in studied bushing along radial direction (from rod to flange).

In order to simulate all possible states of this study, it has been used COMSOL Application Builder module. By programming in this module, the moisture distributions of the studied bushing layers were extracted from an EXCEL table and the results exported to the EXCEL output file. As the Fig. 4 shows, the simulations have been done for each scenario under all pollution conditions. According to this chart, after preparing the bushing model geometry and physics, at the first loop, it is consumed the bushing internal layers has minimum moisture with no pollution on its the external surface. With this consideration, the dielectric constant and electrical conductivity for internal layers and external pollution layer are calculated according to (3) and (13), then the simulation is run. For the second loop, the moisture distribution is changed based on the second predefined scenario and the dielectric constant and electrical conductivity are calculated for the layers and then the simulation is run again. These steps are performed until the last scenario (S8). After the last simulation, the pollution level changes and becomes heavier, for the new pollution level, all scenarios from S1 to S8 are run again. These steps are performed for all pollution levels.

4.1 Effects of Internal Moisture on Electric Field Distribution

In this section, to simulate the moisture in the studied bushing, its effects on the main electrical parameters of the bushing are simulated. The relationship between moisture and relative permittivity and electrical conductivity in OIP insulations has been discussed in the previous sections. It is assumed that the moisture is penetrated from the flange gasket and it goes to the central parts of internal insulations in bushing. It is mentioned, according to Fick's low (1), water tend to diffuse in the insulating paper and when the time passes, the moisture distribution also changes. Also, according to some experimental works [6], [12], the moisture distribution along the time can be like Fig. 5. Therefore, some scenarios are assumed in this study.

It is assumed the moisture distribution start from stage S1 to S8 (8 scenarios). At the last stage (S8), it is considered the moisture diffuse to all of the insulations and the equilibrium is reached, so the moisture distribution is uniform at this stage. In order to model the un-uniform moisture distribution in bushing OIP layers, the complex relative permittivity equations, presented in section two, have been used to estimate relative permittivity and electric conductivity of each layer properties. For every layer, based on the specified moisture, the parameters εr and σ have been calculated by the equations (3) and (13). After parametrizing all layers of the bushing, the electric field distribution obtained.

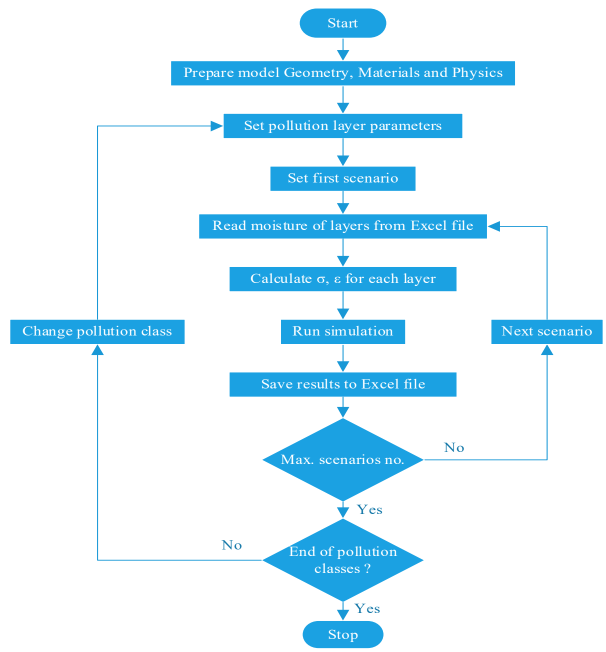

Fig 4. Simulation Flowchart

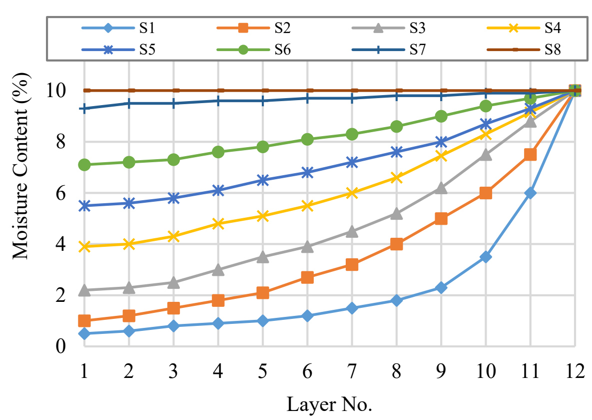

Fig 5. Moisture distribution of layers in the different stages.

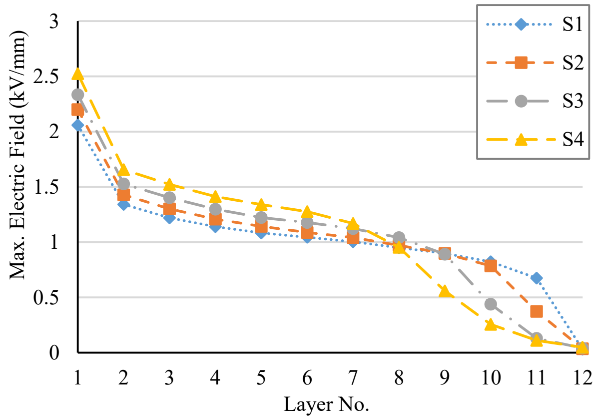

(a) stages 1 to 4

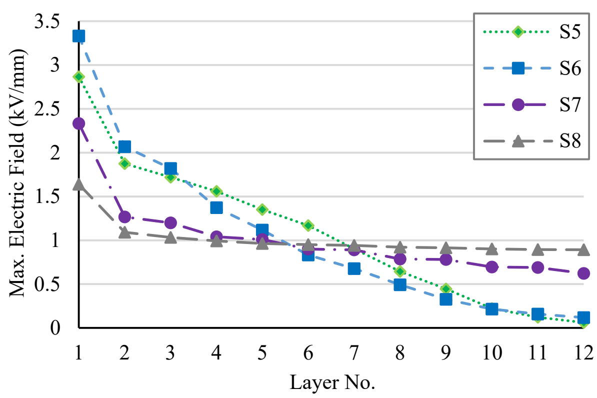

(b) stages 5 to 8

Fig 6. Maximum electric field of layers along radial direction (from rod to flange).

Based on the calculated parameters in each stage, the bushing has been simulated and the electric field values in all layers obtained. Fig. 6 shows the electric field distribution along the radial direction of all layers for stages 1 to 8. As it shows, with passing time and changing the moisture distribution (from S1 to S8), the electric field distribution of layers changes. It can be seen that, by increasing the moisture in layers, the maximum electric field increases, but from 7th stage it is reversed and the maximum electric field decreases. This is due to approaching the bushing to the moisture equilibrium state (approximately equal moisture in all layers); as the moisture get more uniform, the electric field distributes uniformly, even in high moisture contents. Fig. 7 shows the voltage distribution inside the bushing from rod to the last layer. The voltages shown for each layer are measured in the middle of each layer, which is why the first layer is slightly lower than the rod voltage (83.7 kV). As Fig. 7 shows, the moisture distribution has a significant effect on the voltage across the layers.

Fig. 8 shows the maximum electric field of layers for each stage. It can be seen that, stage 6 has the most maximum electric field that created in the OIP insulation in compare with the other stages, and the last stage (S8) lowest maximum electric field due to uniform moisture.

Also, in order to compare the stages in terms of the amount of water penetrated into the insulation, the average moisture content has been calculated in this section. This parameter has been used in the most of the electrical tests for assessing the insulations condition.

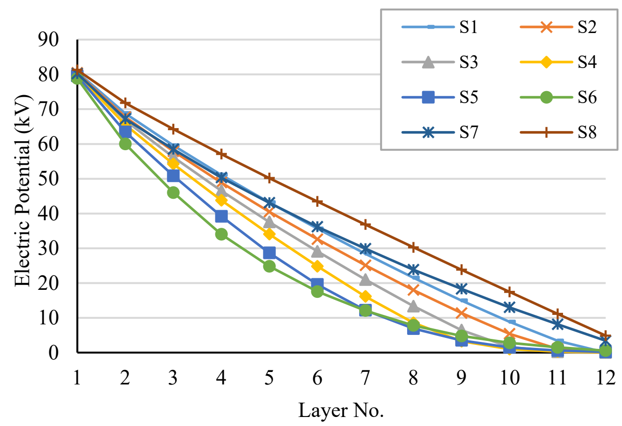

Fig 7. The voltage distribution of layers (middle of each layer) along radial direction.

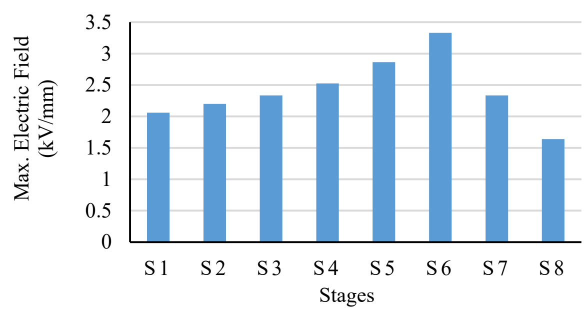

Fig 8. Maximum electric field in OIP at stages 1 to 8

Here, the average moisture content (mc_{av}) is obtained by calculating the weighted average in total OIP insulation. The equation (22) shows how to calculate the average moisture.

$$mc_{av} = \frac{\sum_{i=1}^{12} w_i l_i d_i mc_i}{\sum_{i=1}^{12} w_i l_i d_i} \tag{22}$$

Where, w_i is the weight density of i_{th} layer insulation, l_i is the length of i_{th} layer insulation, d_i is the width of i_{th} layer and mc_i is the moisture content of i_{th} layer.

Table 3 shows the results for each stage compared to the maximum electric field. It can be seen that, increase in moisture content of OIP insulation doesn't have correlation with the maximum electric field in that. Therefore, focusing only on the tests that calculates average moisture content can't help to evaluate bushing internal insulations condition completely.

Table 3. Average moisture content (%) and maximum electric field in OIP at stages S1 to S8

Stage	S1	S2	S3	S4	S5	S6	S7	S8
Average m.c. (%)	1.7	2.8	4.1	5.5	5.7	7.9	9.6	10
Max. electric field(kv/mm)	2.0	2.2	2.3	2.5	2.9	3.3	2.3	1.6

4.2 Effects of Insulator surface Pollution on Internal Electric field Distribution

In this section, the studied bushing has been simulated with different moistures distribution and external surface pollution levels. The pollution has been simulated as a thin layer (width 1mm) along the external surface of bushing insulator (Fig. 9). The properties of this layer have been already defined in Table 4. At pollution levels mentioned in this table, the permittivity of the layer assumed constant, because of low sensitivity on the electric field distribution [27]. Based on the pollution levels as discussed before, the effects of the different pollution levels (light, medium and heavy), on the external and internal insulations of the bushing are evaluated here.

First, the electric potential distribution along the external surface of bushing insulator has been evaluated in all pollution levels without internal moisture. Fig. 10 shows that, as the pollution level gets heavier, the potential distribution gets smoother. The reason is that, the external pollution layer is like an external current path from bushing top cap to the flange; under low pollution condition, this current is almost capacitive (capacitive property), and as the pollution increases, the thin layer becomes a better conductive layer and its current path entering in resistive property.

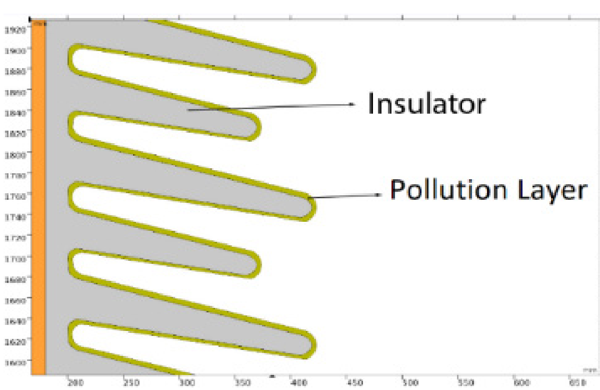

Fig 9. Pollution layer on the studied bushing insulator

In this section, the effects of the external pollutions on electric field distribution in the internal surface of the bushing insulator have been evaluated.

For this purpose, based on the previously mentioned scenarios, the OIP insulations are assumed to contain moisture. The internal surface that electric fields has been measured is shown in the Fig. 11; it is a path in contact with bushing oil. To analyze the effect of the external contaminations, the electric field distribution under each pollution level and without any pollution has been obtained according to Fig.12.

Table 4. Properties of different pollution levels in simulations

Pollution levels	electric conductivity (S/m)	permittivity
Light	$1*10^{-5}$	80
Medium	$1*10^{-3}$	80
Heavy	0.1	80

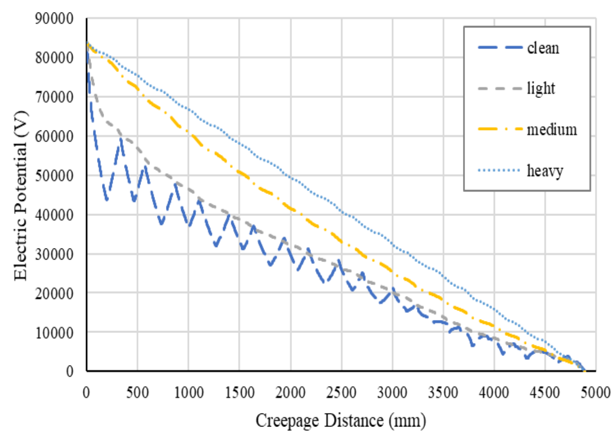

Fig 10. Electric potential distribution along the bushing external insulator under different pollution levels.

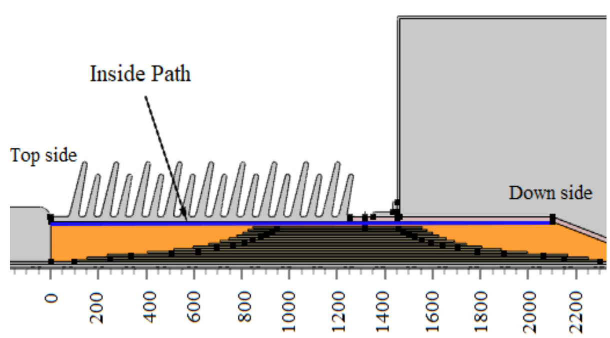

Fig 11. Inside path of bushing (blue color).

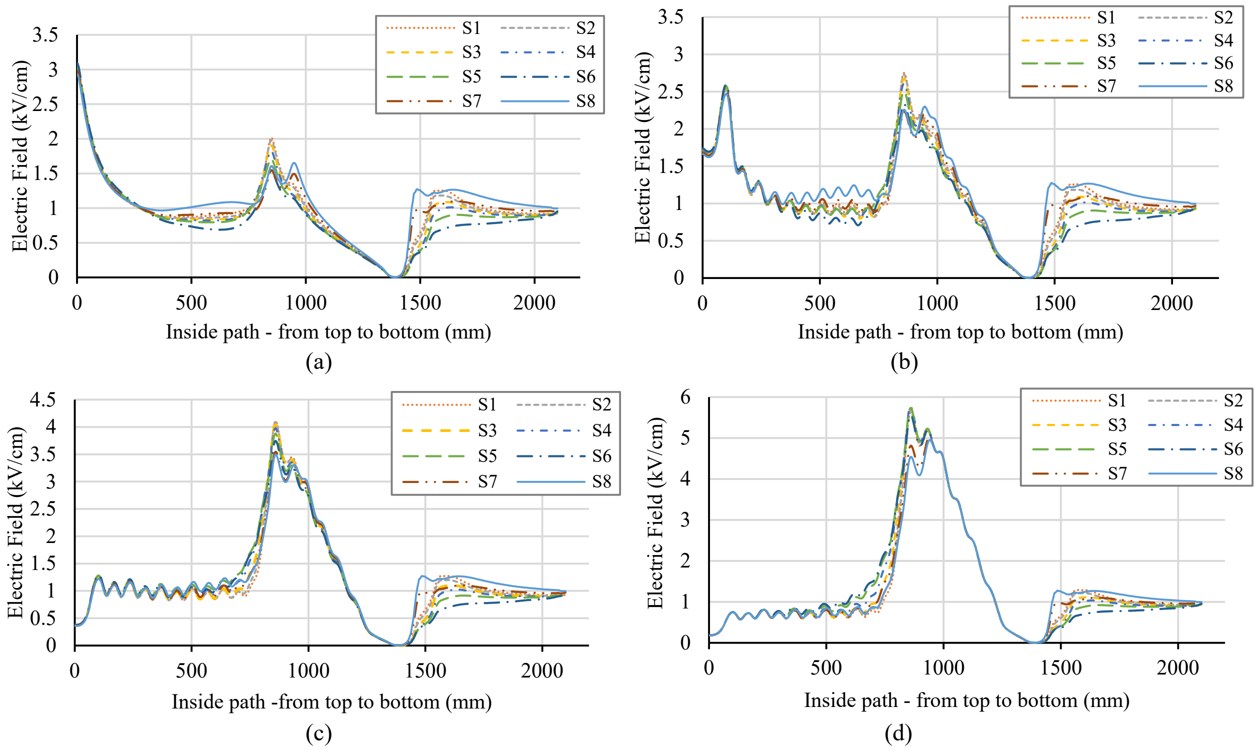

Fig 12. Electric field distribution along inside path of the bushing from stage S1 to S8 under different pollution levels. a) Clean condition, b) Light, c) Medium, d) Heavy

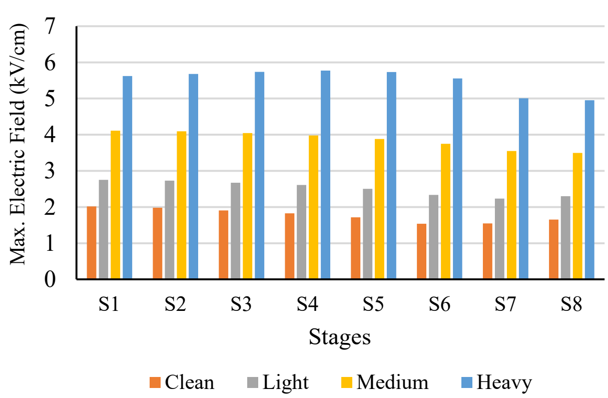

Fig 13. Maximum electric field in inside path, under different pollution levels and scenarios S1 to S8.

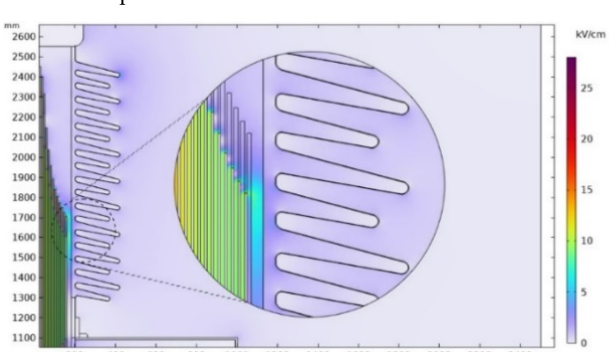

Fig 14. Electric field distribution of the bushing in inside path and under heavy pollution.

Fig. 12-a shows the electric field distribution under clean insulator. It can be seen that, by increasing uniformity of the moisture under different defined scenarios from S1 to S8 in the OIP insulation, themaximum electric field in the middle range of the inside path decreases. That means, the lower moisture leads to more electric field values. This issue can be seen under other pollution levels as well.

Fig. 13 shows the maximum values of the electric field in the internal path of the bushing under different pollution levels. The results show that, with increasing the pollution level on the external surface, the maximum value of the electric field significantly increases. Also, the electric field values of the first scenarios is more than the others. It means, the early stages of moisture penetration into the bushing can be more dangerous than its diffusion in the insulation, from aspect of the electric field.

In Fig. 14, the electric field distribution of the bushing with uniform moisture content is shown under heavy pollution. It shows that the maximum electric field in the inside path occur near the top side of the last OIP layers, especially near the last foil edge. The reason of this peak is overlapping the external electric field that affects from external pollution, and the bushing internal foil edge electric field which affects from internal bushing electric field distribution. Unlike the moisture, which has shown significant effects on the internal electric field of the bushing (as shown in Fig. 6), the simulations showed that the effect of bushing surface pollution is mainly on the electric field of the last layers and has no noticeable effect on the middle and early layers of the bushing.

5 Conclusion

In OIP type bushings, the moisture has tendency to penetrate into insulating system. In this paper, effects of the moisture distribution on the electric fields of the bushing layers have been evaluated. This evaluation has been done by simulating in COMSOL Multiphysics software based on FEM solutions. The results have been shown that as the moisture penetrate to the bushing, the electric field distribution in the OIP insulation is affected and get un-uniform, but with time passing, the moisture in the insulation reaches equilibrium and electric field becomes uniform. So, at the early stages of moisture ingress into the bushing, the maximum electric field of OIP insulations strongly increases (even to twice in compare with uniform moisture distribution), which increase the risk of bushing operation. Also, in this paper, the process of moisture penetration into the bushing has been categorized to 8 stages or scenarios, and the average moisture presented in each stage has been calculated. The results have been shown that the maximum electric field in OIP insulations is not corelated to the average moisture of that, and the distribution of the moisture is important.

Also, the external surface pollution effects on the bushing were studied. The results shown that, when the pollutions severity rises on the bushing surface, the internal electric field of the bushing significantly increases. This affection is more when the moisture penetrates to the bushing especially at the early stages of ingress. It has been shown that, if the distribution of moisture becomes more uneven, the intensity of the electric field on the edges of the last layer's foil of bushing insulation increases and the risk of bushing failure greatly increases.

For future works, the effect of the penetrated moisture on the leakage current of the bushing can also be investigated. In this paper, continuous and uniform pollution effects on the internal electric field of the bushing is considered, but the effect of non-uniform pollution on the electrical field of the bushing can also be investigated in future works.

Conflict of Interest

The authors declare no conflict of interest.

Author Contributions

M. Abouhosseini-Darzi: Research, Software and Simulation, Original Draft Preparation, **M. Mirzaie:** Idea & Conceptualization, Supervision, Analysis, Revise & Editing, Verification, **A. A. Shayegani-Akmal** and **E. Rahimpour**: Advice, Supervision and Verification of the work.

Funding

No funding was received for this work.

References

[1] A. Petersen, "The Risk of transformer fires and strategies which can be applied to reduce the risk," in *CIGRE* Session, Paris, 2010.

[2] W. Youyuan, "Study of the impact of initial moisture content in oil impregnated insulation paper on thermal aging rate of condenser bushing," *Energies*, vol. 8, p. 14298–1431, 2015.

[3] E. Kuffel, *High Voltage Engineering Fundamentals*, Second edition, 2000.

[4] L. Zhou, W. Liao and S. Wang, "A high-precision diagnosis method for damp status of OIP bushing," *IEEE Trans. on Instrumentation and Measurement*, vol. 70, pp. 1-10, 2021.

[5] A. Mikulecky and Z. Štih, "Influence of temperature, moisture content and ageing on oil impregnated paper bushings insulation," *IEEE Trans. on Dielectrics and Electrical Insulation*, vol. 20, no. 4, pp. 1421-1427, Aug. 2013.

[6] L. Zhou, G. Wu and J. Liu, "Modeling of transient moisture equilibrium in oil-paper insulation," *IEEE Trans. on Dielectrics & Electrical Insulation*, vol. 15, no. 3, pp. 872-878, Jun. 2008.

[7] M. Poljak, "Electric field at sharp edge as a criterion for dimensioning condenser-type insulation systems," *Electric Power Systems Research*, vol. 152, p. 485–492, 2017.

[8] H. Yao and e. al., "Evaluation method for moisture content of oil-paper insulation based on segmented frequency domain spectroscopy: From curve fitting to machine learning*," IET Sci. Meas. Technical*, vol. 15, pp. 517-526, 2021.

[9] Q. Dai, Y. Lio and G. Cheng, "Frequency domain spectroscopy for non-uniformly distributed moisture detection in transformer bushings," *IEEE Access*, vol. 8, pp. 210429-210434, 2020.

[10] D. Garcia, "A review of moisture diffusion coefficients in transformer solid," *Electrical Insulation Magazine*, vol. 29, pp. 46-54, 2013.

[11] D. Wang and L.Zhou, "Simulation for transient moisture distribution and effects on the electric field in stable condition: 110kV oil-immersed insulation paper bushing," *IEEE Access*, vol. 7, pp. 162991-163002, 2019.

[12] D. Wang and L.Zhou, "Moisture estimation for oil-immersed bushing based on FDS method- field application," *IET Gener. Transm. Distrib*., vol. 12, no. 11, pp. 2762-2769, 2018.

[13] H. Yao, H. Mu, N. Ding, D. Zhang and Z. Liang, "Evaluation method for moisture content of oil-paper insulation based on segmented frequency

domain spectroscopy: From curve fitting to machine learning," *IET Science, Measurement & Technology*, vol. 15, no. 6, pp. 517-526, 2021.
[14] M. A. Salam, H. Ahmad and T. Tamsir, "Calculation of time to flashover of contaminated insulator by Dimensional Analysis technique," *Computer and Electrical Engineering*, vol. 27, no. 6, pp. 419-427, 2001.
[15] A. Arshad, S. Nekahi, G. McMeekin and M. Farzaneh, "Numerical computation of electric field and potential along silicone rubber insulators under contaminated and dry band conditions," *3D Research*, vol. 7, pp. 1-10, 2016.
[16] J. Zhao, "Effect of external insulation environment on electric field distribution of 500kV porcelain bushing," in *3rd IEEE conference on Energy Internet and Energy System Integration*, Changsha, China, 2019.
[17] E. Akbari, M. Mirzaie, M. Asadpoor and A. Rahimnejad, "Effects of disc insulator type and corona ring on electric field and voltage distribution over 230-kV insulator string by numerical method," *IJEEE*, vol. 9, pp. 58-66, 2013.
[18] B. Qi, Q. Dai and C. Li, "The mechanism and diagnosis of insulation deterioration caused by moisture ingress into oil-impregnated paper bushing," *Energies*, vol. 11, 2018.
[19] C. Ekanayake and S. Gubanski, "Frequency response of oil impregnated pressboard and paper samples for estimating moisture in transformer insulation," *IEEE Trans. on Power Delivery*, vol. 21, no. 3, pp. 1309-1317, 2006.
[20] D. Wang and L.Zhou, "Moisture estimation for oil-immersed bushing based on FDS method at a reference," *IET Gener. Transm. Distrib*., vol. 12, no. 10, pp. 2480-2486, 2018.
[21] Z. Fazarinc, "Computation of electric fields from electric charges: Coulomb's law or poisson's equation," *Comput. Appl. Eng. Educ*., no. 1, pp. 445-454, 1993.
[22] Selection and dimensioning of high-voltage insulators intended for use in polluted conditions-Part1: Definitions, information and general principles, IEC Tech. Spec. 60815-1, 2008.
[23] J. Rasolonjanahary, L. Kräenbühl and A. Nicolas, "Computation of electric fields and potential on polluted insulators using a boundary element method," *IEEE Trans. on Magnetics*, vol. 28, no. 2, pp. 1473-1476, 1992.
[24] E. Asenjo, N. Morales and A. Valdenegro, "Solution of low frequency complex fields in polluted insulators by means of the finite element method," *IEEE Trans. On Dielectric and Electrical Insulation*, vol. 4, pp. 10-16, 1997.
[25] L. Yang, Z. Kuang and e. al, "Study on surface rainwater and arc characteristics of high-voltage bushing with booster sheds under heavy rainfall," *IEEE Access*, vol. 8, pp. 146865-146875, 2020.
[26] M. Akbari, M. Allahbakhshi and R. Mahmoodia, "Heat analysis of the power transformer bushings in the transient and steady states considering the load variations," *Applied Thermal Eng.*, vol. 121, pp. 999-1010, 2017.
[27] J. Araya, "Electric field distribution and leakage currents in glass insulator under different altitudes and pollutions conditions using FEM simulations," *IEEE Latin America Transactions*, vol. 19, no. 8, pp. 278-1285, 2021.

Biographies

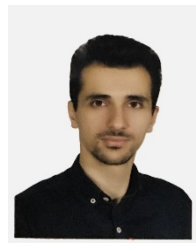

M. Abouhosseini-Darzi was born in Babol, Iran in 1987. He received the B.Sc. degree in electrical power engineering from Zanjan University, Zanjan, Iran in 2009 and M.Sc. degree in electrical power engineering from Isfahan University of Technology, Isfahan, Iran, in 2012. His research interests include high-voltage, Finite Element Method and power transformers insulation systems, testing, and diagnostics.

M. Mirzaie received the B.Sc. degree from Shahid Chamran University, Ahvaz, Iran, in 1997, and the M.Sc. and Ph.D. degrees from the Iran University of Science and Technology, Tehran, Iran, in 2000 and 2007, respectively, all in electrical engineering. He has been a Professor with the Babol Noshirvani University of Technology, Babol, Iran, since 2020. He is the author of more than 120 journal and conference papers. His research interests include high-voltage engineering and also operation problems and condition assessment/monitoring of high-voltage equipment.

A. A. Shayegani-Akmal was born in Tehran, Iran, in 1974. He graduated from the Sharif University of Technology with a B.Sc. degree and from the University of Tehran with a M.Sc. degree in electrical engineering in 1996 and 1998, respectively.,He worked as a Research Assistant at the High Voltage Laboratory of the Sharif University of Technology and University of Tehran. He finished his Ph.D. in electrical engineering through the University of Tehran with cooperation of University of Hanover (Schering-Institute) in 2005. He is currently Associate Professor at the University of

Tehran. His principal research interest is in high-voltage power transformer insulation systems, testing, and diagnostics.

E. Rahimpour (SM'10) received a B.Sc. degree in electrical engineering from Tabriz University in 1993 and M.Sc. and Ph.D. degrees in electrical power engineering from the Faculty of Engineering of Tehran University, Tehran, Iran, in 1995 and 2002, respectively. He was an Associate Professor at the University of Zanjan, working on modeling and monitoring of electrical machines, especially transformers, from 2002 to 2007. He acquired a Georg Forster Research Fellowship of the Alexander von Humboldt Foundation (AvH) Scholarship in 2007 and performed some research involving the transfer function method at the Institute of Power Transmission and High Voltage Technology of Stuttgart University until 2008. He has had several positions, including Director of the Electrical Engineering Department at the University of Zanjan, Program Chairman of the 13th Iranian Conference on Electrical Engineering, the project leader of transformer transients, and responsible for Hitachi transient tools at Hitachi Energy, Transformers, Bad Honnef, Germany. Additionally, he is a member of CIGRE WG A2/C4.39, CIGRE WG A2/C4.52 and Convenor of CIGRE WG A2.63. Currently, he is a professor in the field of electric power systems and network components at the Technical University of Applied Sciences Würzburg-Schweinfurt.